

## Atomic structure of the As-rich InAs(100) $\beta 2(2 \times 4)$ surface

M. Göthelid

Materialfysik, KTH, S-10044 Stockholm, Sweden

Y. Garreau

LURE, CNRS-MENRS-CEA, Bâtiment 209d, Centre Universitaire Paris-Sud, Boîte Postale 34, 91898 Orsay-Cedex, France

M. Sauvage-Simkin

LURE, CNRS-MENRS-CEA, Bâtiment 209d, Centre Universitaire Paris-Sud, Boîte Postale 34, 91898 Orsay-Cedex, France  
and Laboratoire de Minéralogie-Cristallographie, CNRS, Universités Paris 6 et 7, 4 Place Jussieu, 75252 Paris-Cedex 05, France

R. Pinchaux

LURE, CNRS-MENRS-CEA, Bâtiment 209d, Centre Universitaire Paris-Sud, Boîte Postale 34, 91898 Orsay-Cedex, France  
and Université Pierre et Marie Curie, 4 Place Jussieu, 75252 Paris-Cedex 05, France

A. Cricenti

Istituto di Struttura della Materia del CNR, V. E. Fermi 38, 00040 Frascati, Italy

G. Le Lay

CRMC2-CNRS, Case 913, Campus de Luminy, 13288 Marseille Cedex 9, France  
and UFR Sciences de la Matière Université de Provence, Marseille, France

(Received 19 January 1999)

The surface atomic structure of the molecular-beam epitaxy prepared As-rich InAs(100)  $(2 \times 4)$  reconstruction has been solved by synchrotron radiation surface x-ray diffraction. Analysis of a large set of nonequivalent in-plane diffraction peaks and seven out-of-plane rods yields the so-called  $\beta 2(2 \times 4)$  model, a now recognized model for the As-rich GaAs(100)  $(2 \times 4)$  structure. The structure comprises two As dimers in the top layer and one As dimer in the third layer below the first incomplete In layer. [S0163-1829(99)01723-3]

### INTRODUCTION

The atomic structure of the surface reconstructions on (100) surfaces of III-V compound semiconductors has been under investigation for twenty years since Cho published his pioneering work on the GaAs(100) surface.<sup>1</sup> Many questions still remain unsolved, or are still under debate, despite these years of scientific efforts. In many cases, this is related to varying preparation conditions and to the fact that many, more or less, similar geometries yield identical periodic supercells.

GaAs is the most prominent substrate in molecular-beam epitaxy (MBE) growth of III-V structures. The usual growth conditions have focused the attention on the As-stabilized surface structures  $(2 \times 4)/c(2 \times 8)$  [described as  $\alpha$ ,  $\beta$ , and  $\gamma$  phases according to their respective reflection high-energy electron diffraction (RHEED) patterns by Farrell and Palmstrom<sup>2</sup>] and  $c(4 \times 4)$ , with a higher As coverage in the  $c(4 \times 4)$  structure. A recent systematic investigation by Hashizume *et al.*<sup>3</sup> using RHEED and scanning tunnelling microscopy (STM) on MBE grown GaAs(100) surface structures correlated the occurrence of each structure with a given range of annealing temperatures under  $\text{As}_4$  flux. Annealing at 640 °C produces the  $\alpha(2 \times 4)$  phase, 540–630 °C gives the most ordered structure, referred to as the  $\beta$  phase, 510 °C annealing yields the  $\gamma$  phase and finally 490 °C is used to obtain the  $c(4 \times 4)$  structure. Annealing the  $c(4 \times 4)$  surface

without As flux also produced the low-As coverage structures. However, contrary to the assumptions of Farrell and Palmstrom,<sup>2</sup> they concluded that all  $(2 \times 4)$  phases on GaAs (001) present the same structural unit; two As dimers and two dimer vacancies in the top layer. No information could be obtained by STM on the structural features possibly present in the deeper layers.

Since the  $\alpha$ ,  $\beta$ ,  $\gamma$  notation is still broadly referred to in experimental and theoretical works dealing with  $2 \times 4$  reconstructed III-V (100) surfaces it is worth recalling the detailed features of these models. The  $\alpha$  model [Fig. 1(a)] is a two As dimer model with an As surface coverage of 0.5 ML in the top layer. In addition, a Ga dimerization takes place below the missing As dimers in the full-Ga second layer. The  $\beta$  model agrees with the  $\beta 2(2 \times 4)$  model proposed by Chadi,<sup>4</sup> see Fig. 1(b), with two top layer As dimers on top of an, in this case, incomplete Ga layer. The two top layer As dimers are here accompanied by an As dimer in the third layer. The As surface coverage is 0.75 ML. A long-standing hypothesis for the GaAs  $2 \times 4$  surface was a three As dimer model also proposed by Chadi,<sup>4</sup> often referred to as the  $\beta 1(2 \times 4)$  or in short the  $\beta(2 \times 4)$ . Finally, the  $\gamma$  model combines features of the  $\beta 1(2 \times 4)$  phase and of the  $c(4 \times 4)$  phase at higher As coverage,<sup>3</sup> since it can be constructed with an As dimer chemisorbed on a  $\beta 1(2 \times 4)$  surface. All later STM experiments<sup>3,5,6,7</sup> agree on the two As-dimer  $(2 \times 4)$  structures. Furthermore, recent theoretical calculations<sup>8,9,10</sup> also

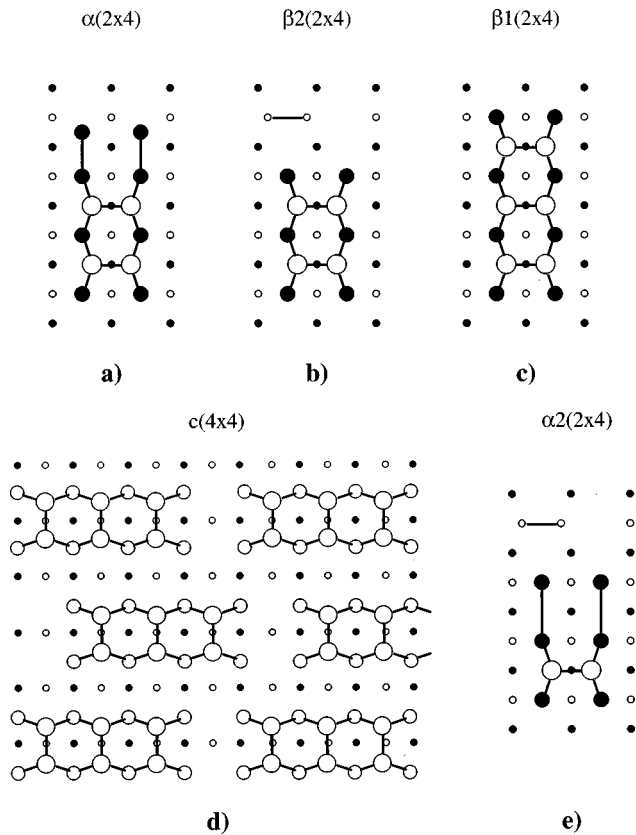


FIG. 1. Geometrical structure models proposed for the group-V rich (100) surfaces. Open circles represent group-V atoms and filled circles group-III atoms.

support this conclusion in favor of a two As dimer  $\beta 2(2 \times 4)$  structure, see Fig. 1(b), which contains blocks of two group-V dimers on top of missing row group-III layer.

A recent surface x-ray diffraction study of the As-terminated GaAs(001)  $(2 \times 4)$  reconstruction, prepared under optimized molecular-beam epitaxy (MBE) conditions,<sup>11</sup> fully confirmed the Chadi  $\beta 2(2 \times 4)$  geometry with two As dimers in the top layer on top of an incomplete Ga layer and an additional As dimer in the third layer and established that the supposed other “phases” were merely due to a larger density of kink defects in the surface order. Models containing three dimers were ruled out.

The  $c(4 \times 4)$  structure was found by SXRD (Ref. 12) and STM (Ref. 13) to consist of triplets of As dimers chemisorbed on a full layer of As, and a similar feature was observed on the  $c(4 \times 4)$  reconstruction on the antimony rich InSb(100) surface.<sup>14,15</sup> The proposed structural model for the  $c(4 \times 4)$  reconstruction is shown in Fig. 1(d).

The InAs(100) surface displays a similar phase diagram with an In-rich  $(4 \times 2)$  structure and two As-rich structures;  $(2 \times 4)$  (Ref. 6) and  $c(4 \times 4)$ .<sup>16</sup> An STM study by Yamaguchi and Hirokoshi,<sup>6</sup> showed that the basic unit for this surface structure indeed also contains two As dimers. Under As-deficient conditions they also observed single As dimers for which they proposed the  $\alpha 2(2 \times 4)$  model, see Fig. 1(e), which contains one As dimer and a dimerization of the second-layer In. In addition an As dimer, similar to the one in the  $\beta 2(2 \times 4)$  model, is present in the third layer.

We have performed surface x-ray diffraction on the MBE-

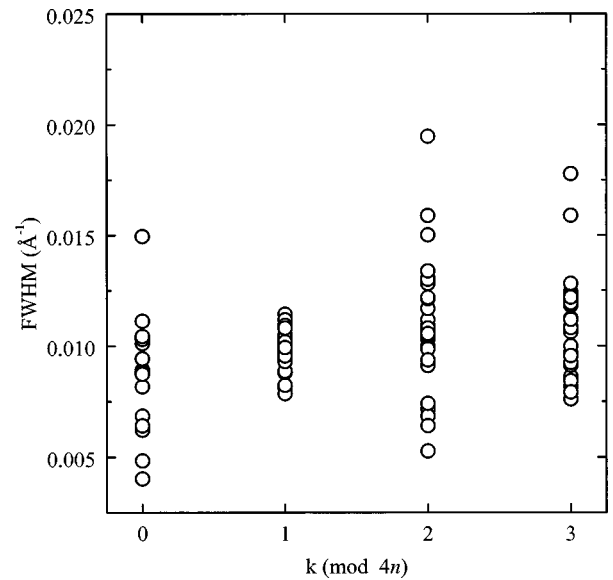


FIG. 2. Histogram of the FWHM of both integer and fractional order diffraction peaks.

prepared As-rich InAs(100)  $(2 \times 4)$  reconstruction in order to determine the full three-dimensional surface geometry. The  $\beta 2(2 \times 4)$  structure yields the best agreement with our experimental data in congruence with recent STM findings.<sup>6</sup>

## EXPERIMENTAL DETAILS

InAs(100) substrates were first cleaned *in situ* by sputtering (500 V,  $5 \times 10^{-5}$  mbar Ar) and annealing (480 °C) cycles until a sharp  $(4 \times 2)/c(8 \times 2)$  low-energy electron diffraction (LEED) pattern was observed. In order to produce the  $(2 \times 4)$  structure the sample was annealed under an As flux (pressure  $2 \times 10^{-6}$  mbar) up to about 350 °C until the fourth order streaks typical of the  $(2 \times 4)$  reconstruction appeared in the  $[\bar{1}10]$  azimuth of the RHEED pattern. After a final LEED control of the surface the sample was transferred, under UHV, onto the diffractometer stage. The surface normal was aligned with the  $\phi$  axis (coincident here with the  $\theta$  axis) by means of a laser beam. The UHV diffractometer is installed on the superconducting wiggler beamline DW12 of the DCI storage ring at LURE (Orsay). Data were collected with focused radiation at  $\lambda = 0.886 \text{ \AA}$ , with the incident beam set at the critical angle for total external reflection, resulting in 58 independent fractional in-plane structure factors. Seven fractional diffraction rods were measured up to a perpendicular momentum transfer  $q_{\perp} = 3.6 \text{ \AA}^{-1}$ . Half-order reflections from the  $\times 2$  periodicity in the  $[\bar{1}10]$  direction were too diffuse to be measured.

Data analysis and structural refinement were performed by using the codes ANA and ROD written by Elias Vlieg. Corrections specific to the  $z$ -axis geometry of the instrument have been applied, taking into account the variations of the Lorentz and polarization factors and of the active sample area.<sup>17</sup>

## RESULTS AND DISCUSSION

An important feature of a reconstructed surface is the size of the coherent domains, which can be derived from the full

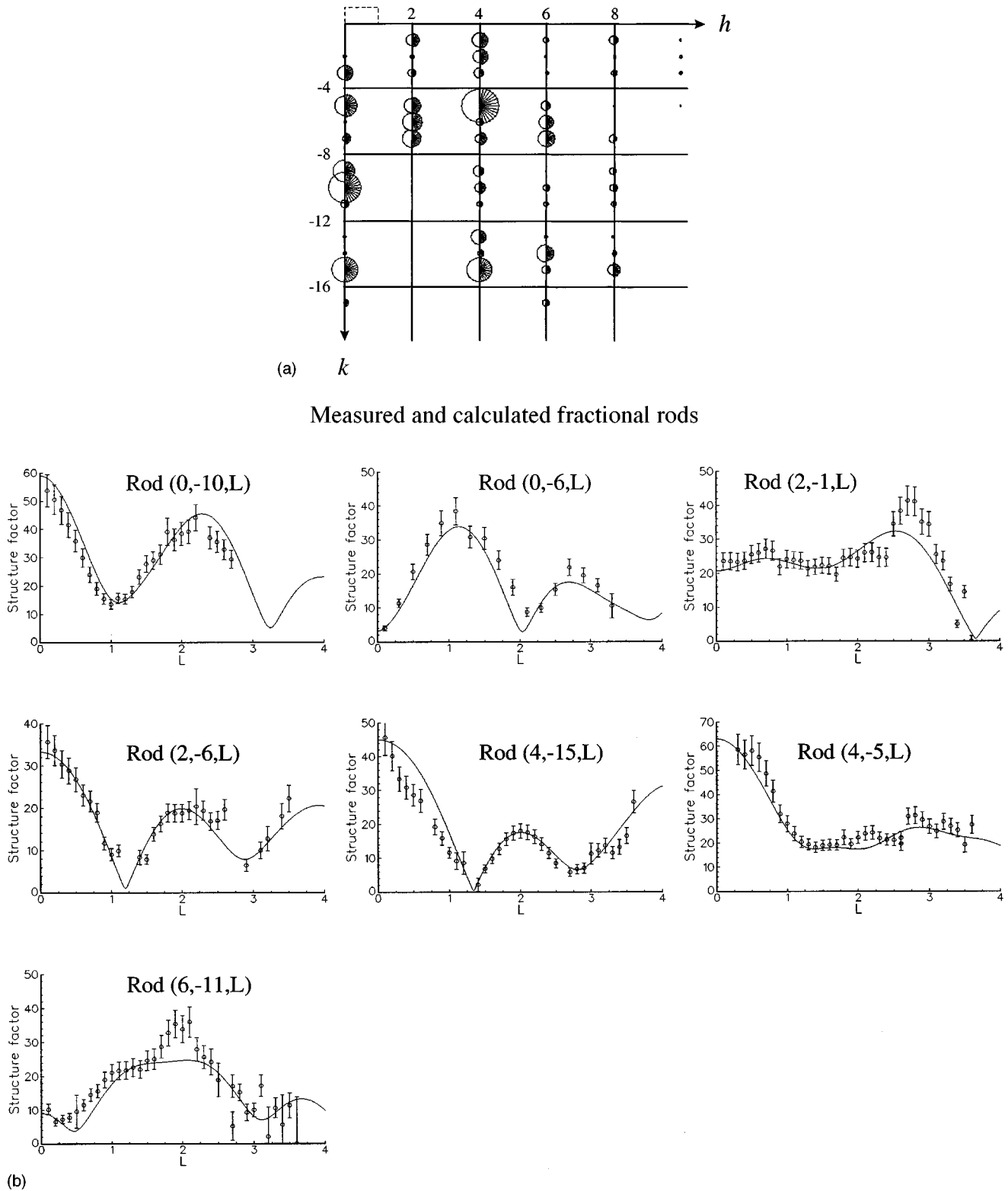


FIG. 3. (a) Graphical presentation of the measured and calculated in-plane structure factors for the  $\beta 2(2 \times 4)$  model. (b) Measured and calculated rod intensities presented as a function of the vertical momentum,  $L$ . The vertical bars indicate the experimental errors.

width at half maximum (FWHM) of the fractional diffraction peaks. For the GaAs(100)  $(2 \times 4)$  surface the half-order peaks had a FWHM twice as large as the quarter-order one that was assigned to the presence of kinks in the As dimer rows.<sup>11</sup> Such a difference in FWHM is not observed in the present case, as can be seen from the FWHM histogram in Fig. 2. Both fractional and integer order spots have approxi-

mately the same average FWHM, around  $9 \times 10^{-3} \text{ \AA}^{-1}$ , although the dispersion is somewhat larger for half orders. The resulting reconstructed domain size ( $2\pi/\text{FWHM}$ ) is  $650 \text{ \AA}$  and appears only limited by the terrace dimensions with a low density of kinks. This result is in agreement with the findings of Yamaguchi *et al.*<sup>18</sup> who derived from STM measurements that the kink density was a factor of 5 lower on

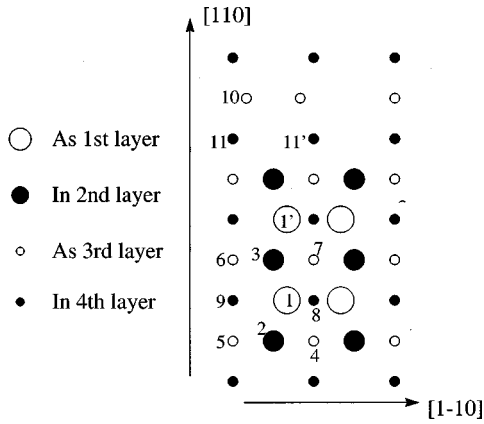


FIG. 4. Detailed drawing of the  $\beta 2(2 \times 4)$  model, defining distances and atoms discussed in the text.

the InAs(100)  $2 \times 4$  surface than on the GaAs(100)  $2 \times 4$  surface.

The models presented in Fig. 1 were all tested in the refining process to select the one most correctly describing this surface structure. The “goodness of fit” was determined in two ways, either by the  $R$  factor defined as

$$R = \frac{\sum (F_{\text{obs}} - |F_{\text{calc}}|)^2}{\sum F_{\text{obs}}^2}$$

or by the residual error  $\chi^2$  defined as

$$\chi^2 = \frac{1}{N-p} \sum \frac{(F_{hkl}^{\text{obs}} - |F_{hkl}^{\text{calc}}|)^2}{\sigma_{hkl}^2},$$

where the  $F$ 's are the measured and calculated structure factors, respectively.  $N$  is the number of inequivalent data points and  $p$  is the number of parameters used in the fitting procedure. The  $\beta 1$  three dimer model does not give a good agreement, neither does the “two As dimer and two In dimer”  $\alpha 1$  model. For the  $\beta 2(2 \times 4)$  structure the final  $R$  factor is 0.15 and  $\chi^2$  equals 2.4, the corresponding numbers for the  $\alpha 2(2 \times 4)$  structure are  $R=0.18$  and  $\chi^2=3.4$ . A graphic representation of the measured and calculated structure factors for the  $\beta 2(2 \times 4)$  model is presented in Fig. 3. The in-plane data are shown in Fig. 3(a) and the out-of-plane structure factor rods

are shown in Fig. 3(b). The  $h$  and  $k$  indices are given with respect to the reconstructed  $(2 \times 4)$  unit cell, indicated in the top left corner of Fig. 3(a).

A detailed drawing of the  $\beta 2(2 \times 4)$  model is shown in Fig. 4, where the different atoms are identified by numbers. Empty circles represent As atoms and filled circles In, with decreasing radius of the circle as the distance from the surface increases. The atomic coordinates are tabulated in Table I. Selected bondlengths and atomic displacements are tabulated in Table II, and compared with data obtained from the GaAs(100)  $(2 \times 4)$  surface by Garreau *et al.*<sup>11</sup> and theoretical results from reference.<sup>19</sup>

Arsenic dimer formation appears to be one of the strong driving mechanisms for this surface reconstruction. The As dimer bondlengths are the same, within the error bars, as those on the GaAs(100)  $(2 \times 4)$  surface, 2.47 Å for the two upper and 2.44 Å for the lower one. As a consequence of the dimerisation does the As(1)-In(2) bondlength increase from the ideal 2.62 to 2.70 Å. The As(1)-In(3) bondlength is even larger, 2.77 Å in agreement with Ref. 8. This is explained by the fact that In(3) has four As neighbors while In(2) is triply coordinated.

Another driving mechanism is that the triply coordinated In atoms at the surface prefer a planar  $sp^2$ -like bonding, previously found from theoretical calculations on the cleavage GaP, InP, GaAs, and InAs (110) surfaces. This tendency drives the In(2) atom away from its “original” bulklike position. The lateral movement is 0.23 Å in the  $\times 4$  direction and 0.68 Å in the  $\times 2$  direction. These values are similar to the corresponding GaAs values.<sup>11</sup> As the In(2) atom moves in between As(1), As(4), and As(5) it pushes the As dimer atoms, As(1), up and away from the surface. In(2) also moves down slightly, again in agreement with GaAs.<sup>11</sup> Further, the As(5) atom is pulled in towards the dimer. The bond angles are indicated in Table I, with the sum being very close to 360°. The deviations from the GaAs surface are obviously due to the difference in lattice parameter for these two surfaces which, since the dimer bondlengths is similar, induces larger strain in the InAs bonds.

The displacements of the indium atoms put strain in the bonds between these indium atoms and the surrounding As. In the top layer the In-As bondlength varies between 2.60 and 2.77 Å, whereas the bulk bondlength is 2.62 Å. Similar deviations from the expected bondlength were also found for the InAs(110) surface,<sup>20</sup> where the surface relaxes upon

TABLE I. Atomic coordinates derived from the best fit of the x-ray diffraction data and referred to the  $2 \times 4$  unit cell with  $a=8.5678$  Å,  $b=17.1357$  Å,  $c=6.0584$  Å,  $\alpha=\beta=\gamma=90^\circ$ .

At°	$x + \Delta x$	$y + \Delta y$	$z + \Delta z$
As(1)	$0.30 \pm 0.055 \pm 0.001$	$0.25 + 0.007 \pm 0.001$	$0.75 + 0.055 \pm 0.005$
In(2)	$0.25 + 0.027 \pm 0.001$	$0.125 + 0.040 \pm 0.001$	$0.50 - 0.035 \pm 0.005$
In(3)	$0.25 + 0.021 \pm 0.001$	0.375 Fixed	$0.50 + 0.018 \pm 0.005$
As(4)	0.50 Fixed	$0.125 - 0.008 \pm 0.001$	$0.25 - 0.032 \pm 0.005$
As(5)	0.00 Fixed	$0.125 + 0.002 \pm 0.001$	$0.25 + 0.037 \pm 0.005$
As(6)	0.00 Fixed	0.375 Fixed	$0.25 - 0.016 \pm 0.005$
As(7)	0.50 (Fixed)	0.375 Fixed	$0.25 + 0.025 \pm 0.005$
As(10)	$0.10 + 0.010 \pm 0.001$	0.875 Fixed	$0.25 + 0.049 \pm 0.005$
In(11)	$0.00 + 0.021 \pm 0.001$	$0.75 - 0.011 \pm 0.001$	$0.00 + 0.020 \pm 0.005$

TABLE II. Comparison of structural parameters from the present study and from the GaAs(001) ( $2\times 4$ ) surface, Ref. 11. See Fig. 4 for the identification of the atoms.

	This study	Garreau (Ref. 11)
Bond length (in Å)		
Top dimer As(1)	2.47	2.51
Bottom dimer As(10)	2.44	2.49
In(2)-As(4)	2.60	2.37
In(2)-As(5)	2.72	2.46
As(1)-In(2)	2.70	2.36
As(1)-In(3)	2.77	2.51
In(11)-As(10)	2.61	2.37
In(11)-In(11')	3.97	3.70
$\Delta z$ (in Å)		
As(1)-In(2)	2.09	1.77
As(4)-As(5)	0.42	0.16 (0.25 from Ref. 19)
As(6)-As(7)	0.25	0.31 (Ref. 19)
Angle (in°)		
As(1)-In(2)-As(4)	117.4	113.5
As(4)-In(2)-As(5)	110.0	112
As(1)-In(2)-As(5)	132.1	133.5

cleavage involving a large outward movement of the surface As atoms and inward relaxation of the In atoms at the surface producing a ‘‘height’’ difference between the In and As atoms of around 0.7 Å. The tilt angle of the In-As bond at the surface being up to 30°.

The atomic structure of the GaAs(100)  $\beta 2(2\times 4)$  surface was recently derived by *ab initio* calculations.<sup>19</sup> A vertical buckling of the As atoms in the third layer [As(4), As(5), As(6), and As(7)] were observed.<sup>19</sup> The values found in that study are tabulated in Table II and compared with values found here in this experiment. The values are similar, with a slightly larger height difference between the As(4) and As(5) atoms here. This is again related to the fact that the larger InAs lattice requires larger absolute displacements of the atoms to relax around the As dimers.

## CONCLUSIONS

We have studied the As-terminated InAs(100)  $\beta 2(2\times 4)$  reconstruction using surface x-ray diffraction. The full three dimensional geometry has been determined, which consists of two As dimers in the top layer and one As dimer in the third layer as for the corresponding GaAs(100) ( $2\times 4$ ) superstructure. A buckling of the third layer As atoms below the top layer As dimers is also reported, in agreement with recent theoretical result on the GaAs(100) surface.

## ACKNOWLEDGMENTS

We thank the LURE staff for creating an excellent atmosphere and for providing equivalently excellent experimental conditions. EC funding under Contract No. CII\*-CT93-0034 for the upgrade of the LURE surface diffraction beamline is gratefully acknowledged. One of the authors (M.G.) thanks the Swedish Board for Natural Sciences (NFR) for financial support.

<sup>1</sup>A. Y. Cho, J. Appl. Phys. **47**, 2841 (1976).

<sup>2</sup>H. H. Farrell and C. J. Palmstrom, J. Vac. Sci. Technol. B **8**, 903 (1990).

<sup>3</sup>T. Hashizume, Q. K. Xue, A. Ichimiya, and T. Sakurai, Phys. Rev. B **51**, 4200 (1995).

<sup>4</sup>D. J. Chadi, J. Vac. Sci. Technol. A **5**, 834 (1987).

<sup>5</sup>J. Zhou, Q. Xue, H. Chaya, T. Hashizume, and T. Sakurai, Appl. Phys. Lett. **64**, 583 (1994).

<sup>6</sup>H. Yamaguchi and Y. Horikoshi, Phys. Rev. B **51**, 9836 (1995).

<sup>7</sup>A. R. Avery, D. M. Holmes, and T. S. Jones, Surf. Rev. Lett. **1**, 621 (1994).

<sup>8</sup>W. G. Schmidt and F. Bechstedt, Surf. Sci. **360**, L473 (1996).

<sup>9</sup>K. Shiraishi and T. Ito, Surf. Sci. **357–358**, 451 (1996).

<sup>10</sup>J. E. Northrup and S. Froyer, Mater. Sci. Eng., B **30**, 81 (1995).

<sup>11</sup>Y. Garreau, M. Sauvage-Simkin, N. Jedrecy, R. Pinchaux, and M. B. Veron, Phys. Rev. B **54**, 17 638 (1996).

<sup>12</sup>M. Sauvage-Simkin, R. Pinchaux, J. Massies, P. Paverie, J. Bonnet, N. Jedrecy, and I. K. Robinson, Phys. Rev. Lett. **62**, 563 (1989).

<sup>13</sup>D. K. Biegelsen, R. D. Bringans, J. E. Northrup, and L. E. Swartz, Phys. Rev. B **41**, 5701 (1990).

<sup>14</sup>C. F. McConville, T. S. Jones, F. M. Leibsle, S. M. Driver, T. C. Q. Noakes, M. O. Schweitzer, and N. V. Richardson, Phys. Rev. B **50**, 14 965 (1994).

<sup>15</sup>C. F. McConville, T. S. Jones, F. M. Leibsle, and N. V. Richardson, Surf. Sci. **303**, L373 (1994).

<sup>16</sup>C. Ohler, C. Daniels, A. Förster, and H. Lüth, J. Vac. Sci. Technol. B **15**, 702 (1997).

<sup>17</sup>M. B. Veron, Ph.D thesis, Université Pierre et Marie Curie, Paris, 1996; O. Robach, Y. Garreau, K. Aid, and M. B. Vernon (unpublished).

<sup>18</sup>H. Yamaguchi and Y. Horikoshi, Phys. Rev. B **53**, 4565 (1996).

<sup>19</sup>G. P. Srivastava, and S. J. Jenkins, Surf. Rev. Lett. **5**, 219 (1998).

<sup>20</sup>J. L. A. Alves, J. Hebenstreit, and M. Scheffler, Phys. Rev. B **44**, 6188 (1991), and references therein.